Article:
Lord, RM, Zegke, M, Basri, AM et al. (2 more authors) (2021) Rhodium(III) Dihalido Complexes: The Effect of Ligand Substitution and Halido Coordination on Increasing Cancer Cell Potency. Inorganic Chemistry, 60 (3). pp. 2076-2086. ISSN 0020-1669

https://doi.org/10.1021/acs.inorgchem.0c03704

Rhodium(III) dihalido complexes: the effect of ligand substitution and halido coordination on increasing cancer cell potency

Rianne M. Lord,[a,b]* Markus Zegke,[b] Aida M. Basri,[c] Christopher M. Pask[c] and Patrick C. McGowan[c]

[a] School of Chemistry, University of East Anglia, Norwich Research Park, Norwich, NR4 7TJ, U.K. Email: r.lord@uea.ac.uk

[b] School of Chemistry and Biosciences, University of Bradford, Bradford, BD7 1DP, U.K.

[c] School of Chemistry, University of Leeds, Woodhouse Lane, Leeds, LS2 9JT, U.K.

X-ray Crystallographic Analysis

Table S 1 X-ray crystallographic data for complexes **1**, **3 (Δ and Λ)**, **4a** and **4b**, s.u.s shown in parenthesis

Complex	1	3 (Δ)	3 (Λ)	4a	4b
CCDC Number	1978080	1978078	2042715	1978082	1978081
Empirical formula	$C_{25}H_{21}Cl_2F_2N_4O_3Rh$	$C_{24}H_{17}Br_2Cl_2N_4O_2Rh$	$C_{24}H_{17}Br_2Cl_2N_4O_2Rh$	$C_{26}H_{25}Cl_2I_2N_4O_4Rh$	$C_{27}H_{24}Cl_2I_2N_5O_3Rh$
Formula weight	637.278	727.046	727.046	885.132	894.143
Temperature/K	100.1(4)	99.9(3)	100.3(9)	100.2(4)	120.3(7)
Crystal system	orthorhombic	monoclinic	monoclinic	monoclinic	monoclinic
Space group	$P2_12_12_1$	Cc	Cc	$P2_1/c$	$P2_1/n$
a/Å	10.5456(3)	9.3613(3)	9.3527(2)	17.9801(8)	8.1441(3)
b/Å	12.0060(4)	23.8677(7)	23.9723(6)	10.3200(4)	32.8058(12)
c/Å	19.5775(7)	11.4997(3)	11.5084(3)	17.7408(9)	11.0381(4)
α/°	90	90	90	90	90
β/°	90	100.495(3)	100.627(2)	115.036(6)	90.522(3)
γ/°	90	90	90	90	90
Volume/Å³	2478.72(14)	2526.43(13)	2535.99(11)	2982.6(3)	2948.98(18)
Z	4	4	4	4	4
ρ_{calc}g/cm³	1.708	1.911	1.904	1.971	2.014
μ/mm⁻¹	0.956	4.081	4.065	2.860	23.116
F(000)	1277.3	1411.6	1411.6	1698.2	1729.4
Crystal size/mm³	0.478 × 0.202 × 0.132	0.093 × 0.06 × 0.04	0.21 x 0.15 x 0.09	0.412 × 0.366 × 0.316	0.102 × 0.072 × 0.035
Radiation	Mo Kα (λ = 0.71073)	Mo Kα (λ = 0.71073)	Mo Kα (λ = 0.71073	Mo Kα (λ = 0.71073)	Cu Kα (λ = 1.54184)
2Θ range for data collection/°	6.62 to 59.08	6.42 to 51.36	4.74 to 60.72	6.38 to 59.06	8.46 to 147.42
Index ranges	-14 ≤ h ≤ 10, -15 ≤ k ≤ 15, -19 ≤ l ≤ 27	-8 ≤ h ≤ 11, -25 ≤ k ≤ 28, -14 ≤ l ≤ 14	-11 ≤ h ≤ 12, -23 ≤ k ≤ 31, -14 ≤ l ≤ 12	-24 ≤ h ≤ 20, -13 ≤ k ≤ 14, -24 ≤ l ≤ 24	-9 ≤ h ≤ 9, -38 ≤ k ≤ 40, -13 ≤ l ≤ 13
Reflections collected	9366	6634	6999	19498	13120
Independent reflections	5515 [R_{int} = 0.0438, R_{sigma} = 0.0893]	3782 [R_{int} = 0.0263, R_{sigma} = 0.0397]	5022 [R_{int} = 0.0176, R_{sigma} = 0.0299]	7240 [R_{int} = 0.0499, R_{sigma} = 0.0645]	5776 [R_{int} = 0.0571, R_{sigma} = 0.0721]
Data/restraints/parameters	5515/0/336	3782/2/316	5022/2/316	7240/0/356	5776/0/363
Goodness-of-fit on F²	1.040	1.047	1.022	1.051	1.064
Final R indexes [I>=2σ (I)]	R_1 = 0.0524, wR_2 = 0.1092	R_1 = 0.0228, wR_2 = 0.0513	R_1 = 0.0243, wR_2 = 0.0614	R_1 = 0.0499, wR_2 = 0.0972	R_1 = 0.0565, wR_2 = 0.1339
Final R indexes [all data]	R_1 = 0.0636, wR_2 = 0.1170	R_1 = 0.0238, wR_2 = 0.0519	R_1 = 0.0258, wR_2 = 0.0619	R_1 = 0.0668, wR_2 = 0.1063	R_1 = 0.0707, wR_2 = 0.1438
Largest diff. peak/hole / e Å⁻³	1.38/-0.90	0.47/-0.35	0.78/-0.45	3.04/-2.54	2.14/-1.50
Flack parameter	-0.07(5)	0.017(6)	0.025(5)	--	--

Table S 2 Selected bond angles (°) for complexes **1**, **3 (Δ and Λ)**, **4a** and **4b**, s.u.s shown in parentheses

Bonds	1	3 (Δ)	3 (Λ)	4a	4b
X(1)-Rh(1)-X(2)	92.33(7)	93.00(4)	92.93(3)	90.86(5)	177.88(7)
X(1)-Rh(1)-O(2)	177.09(15)	177.14(8)	177.19(7)	176.28(11)	86.76(16)
X(2)-Rh(1)-O(2)	88.46(13)	86.00(8)	86.09(7)	91.14(11)	91.98(16)
X(1)-Rh(1)-N(1)	89.41(17)	89.02(10)	89.25(9)	89.18(12)	175.3(2)
X(2)-Rh(1)-N(1)	96.79(18)	96.06(10)	96.06(9)	95.31(13)	88.28(18)
X(1)-Rh(1)-N(2)	90.46(18)	90.32(10)	90.50(9)	89.48(13)	90.58(19)
X(2)-Rh(1)-N(2)	175.70(18)	175.11(9)	175.10(9)	175.45(12)	90.60(19)
X(1)-Rh(1)-N(3)	96.85(19)	97.62(10)	97.66(9)	96.48(13)	92.26(18)
X(2)-Rh(1)-N(3)	88.75(17)	86.14(10)	86.09(9)	88.26(13)	89.16(18)
N(1)-Rh(1)-O(2)	93.3(2)	93.74(12)	93.47(11)	93.75(15)	97.7(2)
N(2)-Rh(1)-O(2)	88.9(2)	90.85(13)	90.65(11)	88.78(16)	176.3(3)
N(3)-Rh(1)-O(2)	80.4(2)	79.65(12)	79.66(11)	80.45(15)	78.4(2)
N(1)-Rh(2)-N(2)	80.0(2)	80.40(14)	80.48(12)	80.16(17)	79.7(3)
N(1)-Rh(1)-N(3)	171.5(2)	172.90(13)	172.67(12)	173.27(17)	175.3(2)
N(2)-Rh(1)-N(3)	94.2(2)	96.98(13)	96.92(12)	96.21(17)	104.3(3)

Table S 3 X-ray crystallographic data for complexes **6** and **7**, s.u.s shown in parenthesis

Complex	6	7
CCDC Number	1978079	1978083
Empirical formula	$C_{27}H_{24}Cl_2I_2N_5O_3Rh$	$C_{27}H_{24}Br_2I_2N_5O_3Rh$
Formula weight	894.143	983.045
Temperature/K	100.0(3)	120.2(4)
Crystal system	monoclinic	monoclinic
Space group	Cc	Cc
a/Å	15.4740(11)	15.5643(6)
b/Å	9.1361(6)	9.1945(4)
c/Å	21.4115(13)	21.4844(10)
α/°	90	90
β/°	95.700(6)	95.650(4)
γ/°	90	90
Volume/Å^3	3012.0(4)	3059.6(2)
Z	4	4
ρ_{calc}g/cm^3	1.972	2.134
μ/mm^{-1}	2.832	5.225
F(000)	1714.2	1855.4
Crystal size/mm^3	0.118 × 0.108 × 0.031	0.15 × 0.09 × 0.07
Radiation	Mo Kα (λ = 0.71073)	Mo Kα (λ = 0.71073)
2Θ range for data collection/°	6.22 to 52.74	6.18 to 62.3
Index ranges	-16 ≤ h ≤ 19, -11 ≤ k ≤ 9, -26 ≤ l ≤ 21	-21 ≤ h ≤ 22, -11 ≤ k ≤ 12, -22 ≤ l ≤ 28
Reflections collected	9196	10526
Independent reflections	4805 [R_{int} = 0.0675, R_{sigma} = 0.1033]	6153 [R_{int} = 0.0368, R_{sigma} = 0.0602]
Data/restraints/parameters	4805/98/309	6153/2/363
Goodness-of-fit on F^2	1.052	1.018
Final R indexes [I>=2σ (I)]	R_1 = 0.0512, wR_2 = 0.0906	R_1 = 0.0383, wR_2 = 0.0806
Final R indexes [all data]	R_1 = 0.0675, wR_2 = 0.1016	R_1 = 0.0432, wR_2 = 0.0840
Largest diff. peak/hole / e Å^{-3}	1.01/-0.91	1.00/-0.77
Flack parameter	-0.06(4)	0.040(12)

Table S 4 Selected bond angles (°) for complexes **6** and **7**, s.u.s shown in parentheses

Bonds	6	7
X(1)-Rh(1)-X(2)	177.34(5)	174.38(2)
X(1)-Rh(1)-O(2)	88.1(2)	88.21(14)
X(2)-Rh(1)-O(2)	89.4(2)	86.66(14)
X(1)-Rh(1)-N(1)	89.9(3)	89.13(16)
X(2)-Rh(1)-N(1)	89.5(3)	89.20(14)
X(1)-Rh(1)-N(2)	92.4(3)	91.31(16)
X(2)-Rh(1)-N(2)	90.0(3)	93.63(16)
X(1)-Rh(1)-N(3)	88.4(3)	92.10(15)
X(2)-Rh(1)-N(3)	91.9(3)	89.01(145
N(1)-Rh(1)-O(2)	94.9(4)	96.8(2)
N(2)-Rh(1)-O(2)	174.9(4)	175.7(2)
N(3)-Rh(1)-O(2)	78.2(3)	77.3(2)
N(1)-Rh(2)-N(2)	80.0(4)	79.0(2)
N(1)-Rh(1)-N(3)	173.0(4)	173.9(2)
N(2)-Rh(1)-N(3)	106.7(5)	107.0(2)

Characterization by FTIR and PXRD

FTIR Spectroscopy for Complex 3 Isomers

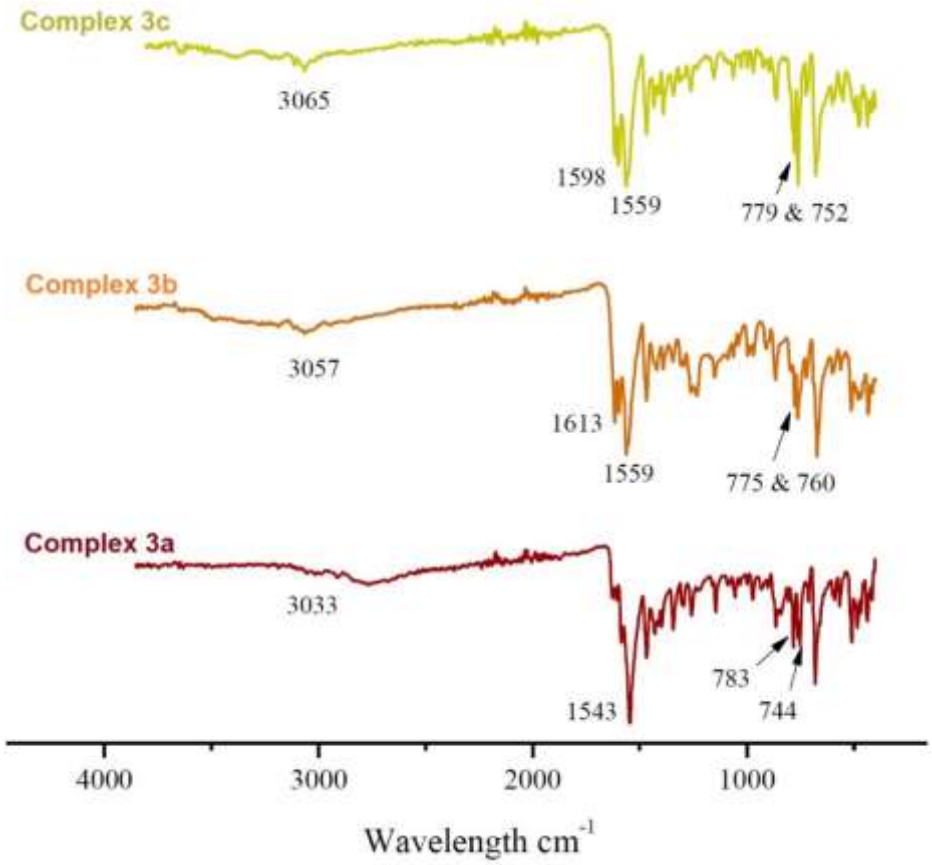

Figure S 1 IR spectra of complexes **3a** (**red**), **3b** (**orange**) and **3c** (**yellow**).

PXRD of Complexes 3 and Complex 7

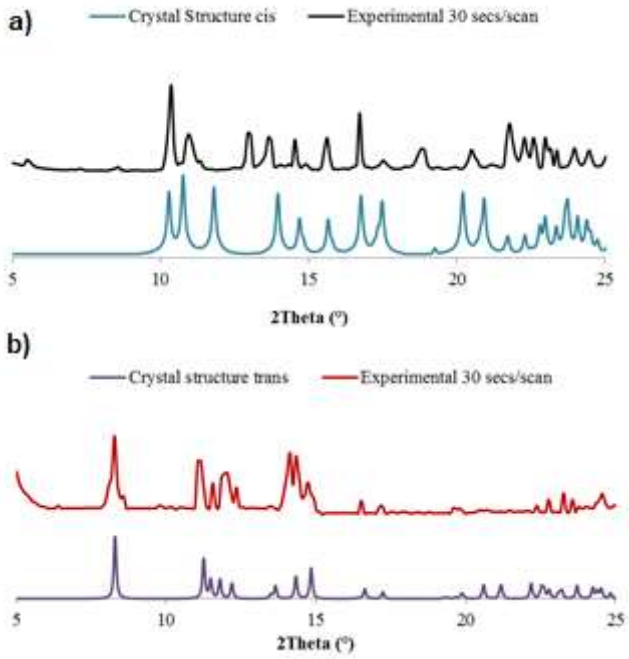

Figure S 2 Simulated and experimental PXRD diffractograms for **a)** complex **3** and **b)** complex **7**.

Characterization NMR Spectroscopy

Complex 3 – 1st synthetic products

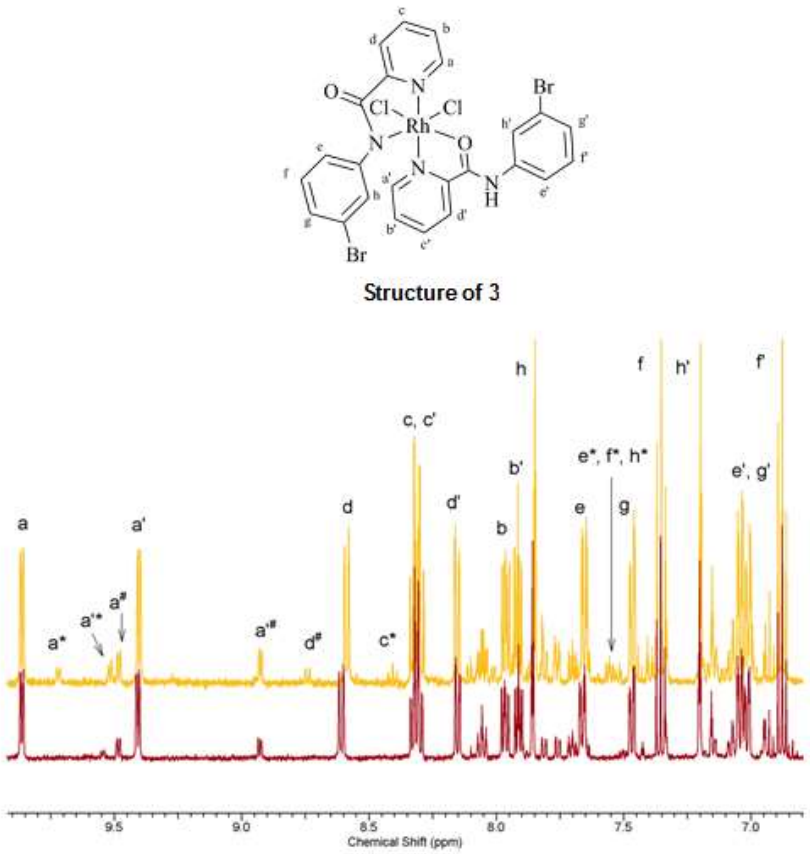

Figure S 3 ^{1}H NMR spectra of complexes **3a** (**red**) and **3c** (**yellow**) (d_6-acetone, 300 K, 300 MHz).

Variable Temperature NMR Spectroscopy of Complex 3 – 1st synthetic product

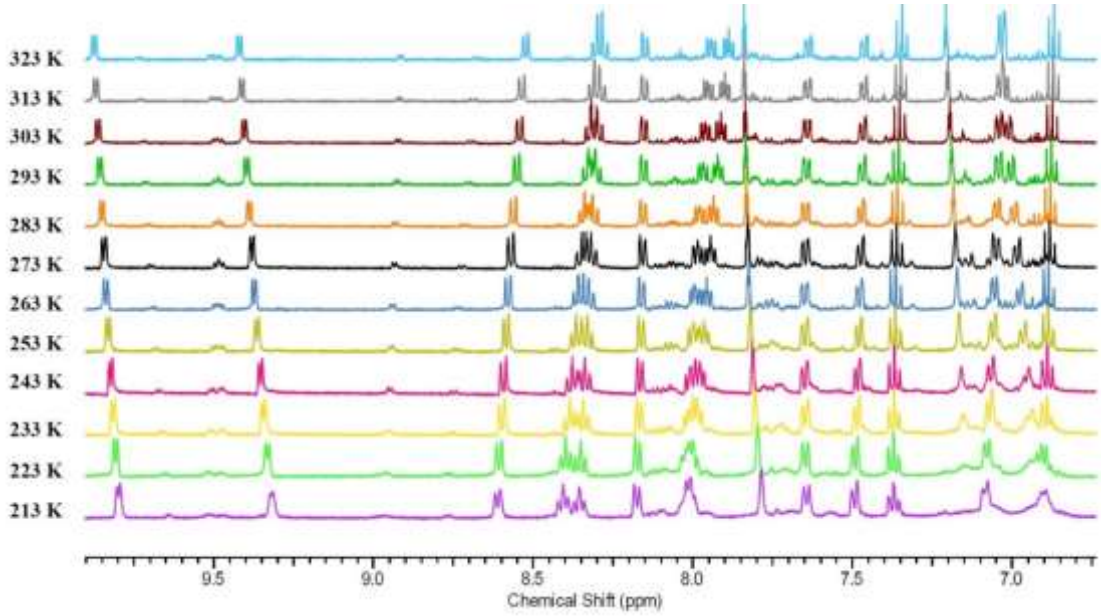

Figure S 4 Temperature-dependent ^{1}H NMR spectra of complex **3c** (d_6-acetone, 300 K, 300 MHz).

NMR for Complex 3 – 2nd synthetic product

Figure S 5 Image of the combined crystals under a microscope

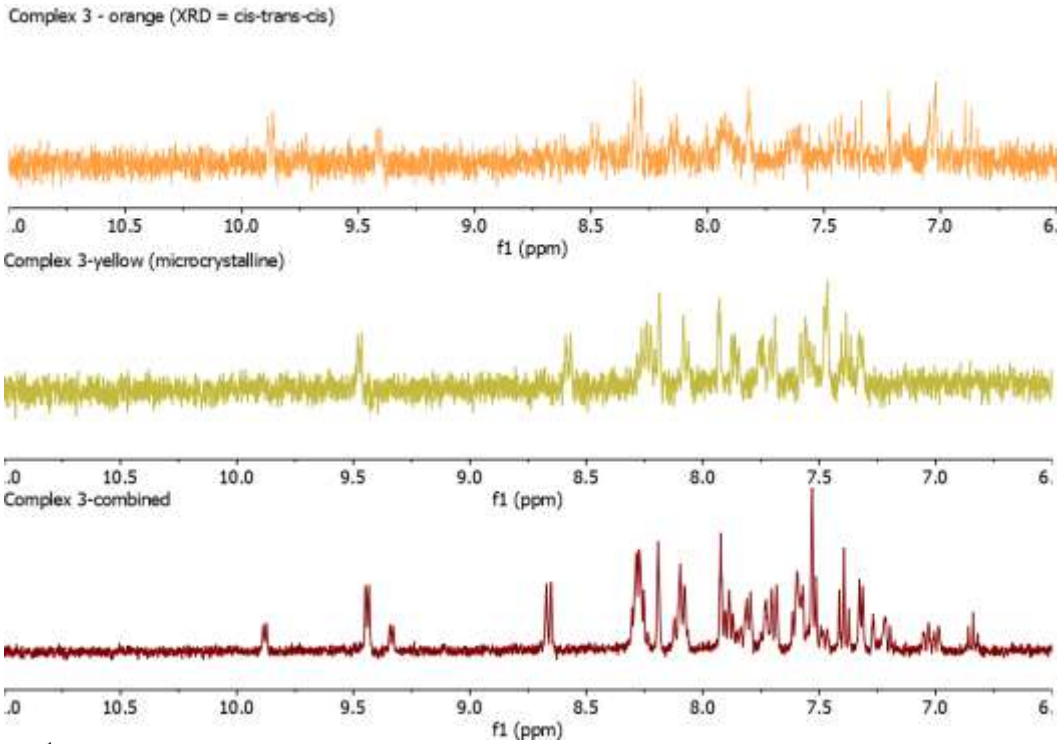

Figure S 6 ^{1}H NMR spectra of complexes **3-combined** (**red**) and **3-yellow microcrystals** and **3-orange single crystals** (d_6-acetone, 300 K, 400 MHz).

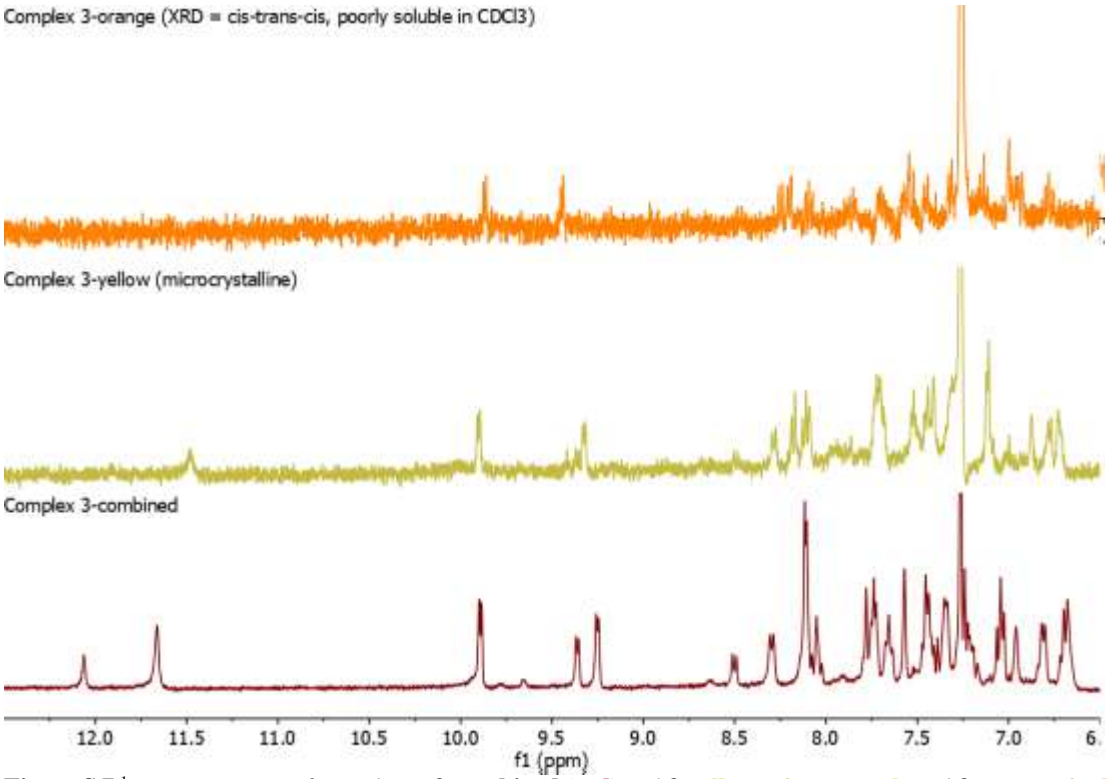

Figure S 7 ^{1}H NMR spectra of complexes **3-combined** (**red**) and **3-yellow microcrystals** and **3-orange single crystals** (CDC_3, 300 K, 400 MHz).

NMR Characterisation and Exchange Studies of Complexes 1, 4, 5 and 8

Comparison NMR spectroscopy of complexes 1 and 5

^{1}H NMR spectra were recorded for **[(3'-F)(3'-FH)RhCl$_2$]** (**1**, **black**) and **[(3'-F)(3'-FH)RhI$_2$]** (**5**, **blue**) (**Figure S4**) at room temperature and show that complex **1** exhibits multiple isomers in solution, whereas complex **5** has only one isomer in solution. This can be clearly observed for the NH proton of the ligand, which appears at a chemical shift of ~12.5 ppm.

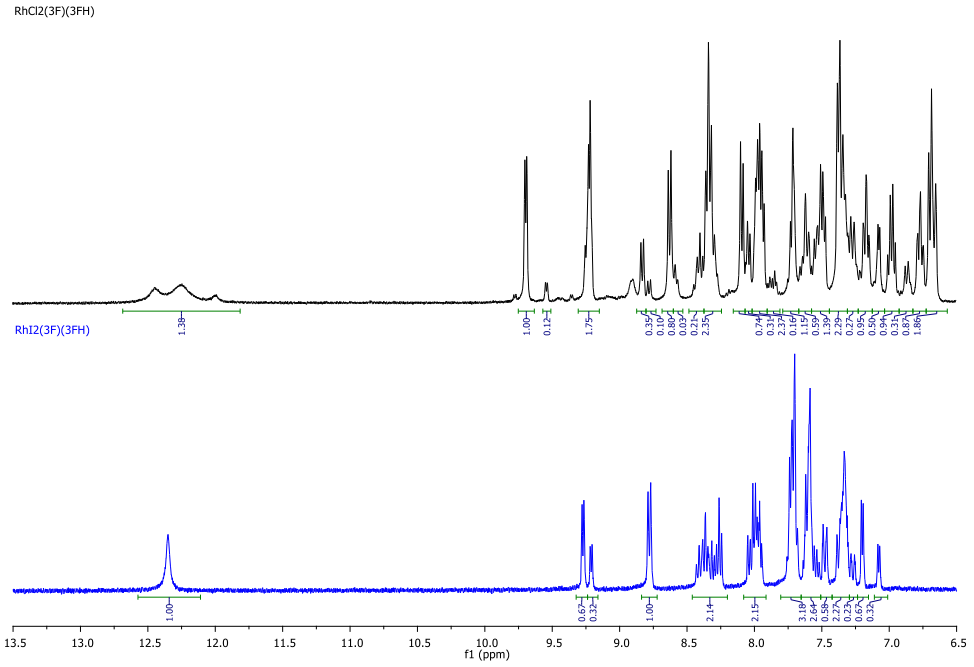

Figure S 8 ^{1}H NMR spectrum of **[(3'-F)(3'-FH)RhCl$_2$]** (**1**, **black**) and **[(3'-F)(3'-FH)RhI$_2$]** (**5**, **blue**) confirming the different number of isomer present ($CDCl_3$, 300 K, 400 MHz)

NMR's in Chloroform

Complex 1 + N-(3-iodophenyl)picolinamide

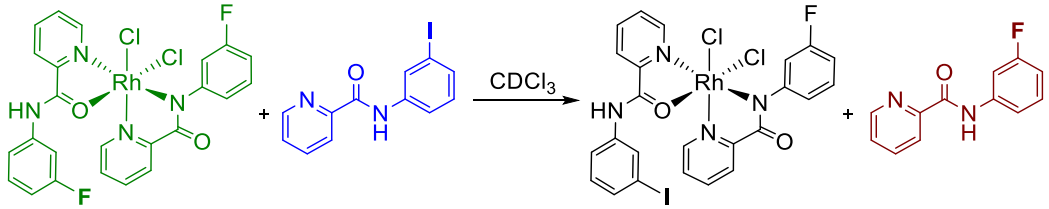

Scheme S1 Ligand exchange of **[(3'-F)(3'-FH)RhCl$_2$]** (**1**) with ligand **3'-IH** in $CDCl_3$.

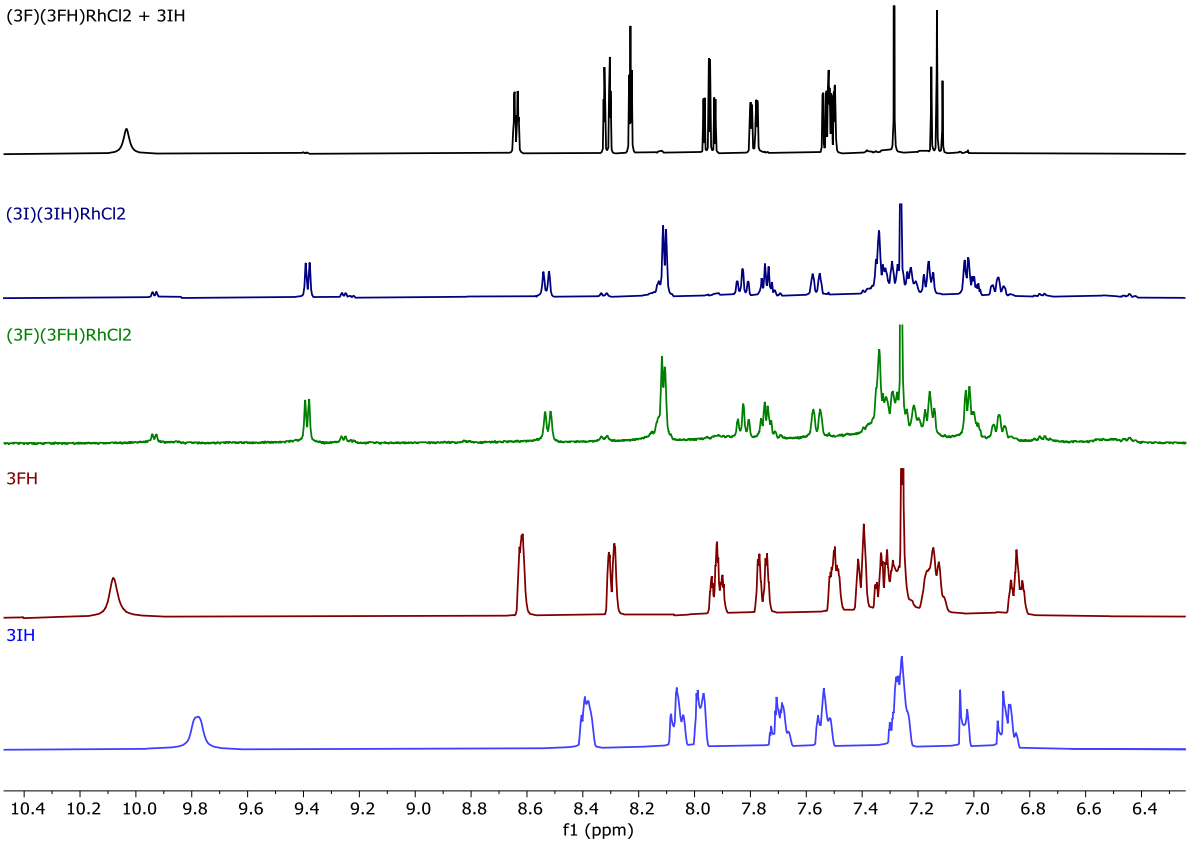

Figure S 9 Overlay of the product (**black**) from the reaction of **[(3'-F)(3'-FH)RhCl$_2$]** (**1**, **dark green**) + ligand **3'-IH** (**blue**). The spectra for **[(3'-I)(3'-IH)RhCl$_2$]** (**4**, **dark blue**) and ligand **3'-FH** (**dark red**) are also included for comparison ($CDCl_3$, 300 K, 400 MHz).

The ^{1}H NMR study of an equimolar mixture of **[(3'-F)(3'-FH)RhCl$_2$] (1)** and ***N*-(3-iodophenyl)picolinamide (3'-IH)** in $CDCl_3$ shows the formation of a mixed species which is possibly **[(3'-F)(3'-IH)RhCl$_2$] or [(3'-FH)(3'-I)RhCl$_2$]** and the dissociation of ***N*-(3-fluorophenyl)picolinamide (3'-FH)**. The resonances of [(3'-L)(3'-LH)RhCl$_2$] are "swamped" by the free ligand due to the complex's poor solubility in $CDCl_3$. In addition, the ^{1}H NMR spectra of **[(3'-F)(3'-FH)RhCl$_2$] (1)** and **[(3'-I)(3'-IH)RhCl$_2$] (4)** are essentially indistinguishable, thus inhibiting a direct *in situ* analysis of a mixed **[(3'-F)(3'-IH)RhCl$_2$] or [(3'-FH)(3'-I)RhCl$_2$]** complex.

Complex 4 + N-(3-fluorophenyl)picolinamide

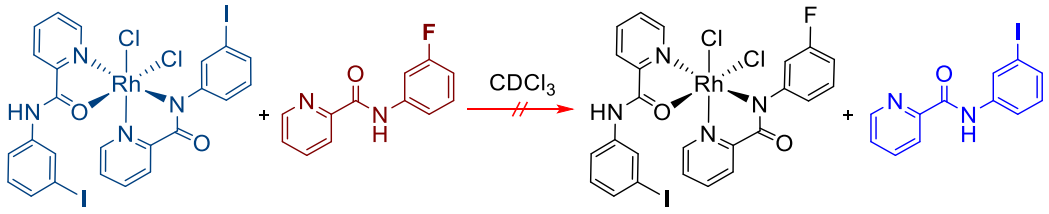

Scheme S2 Attempted ligand exchange of **[(3'-I)(3'-IH)RhCl$_2$]** (**4**) with **3'-FH** in $CDCl_3$.

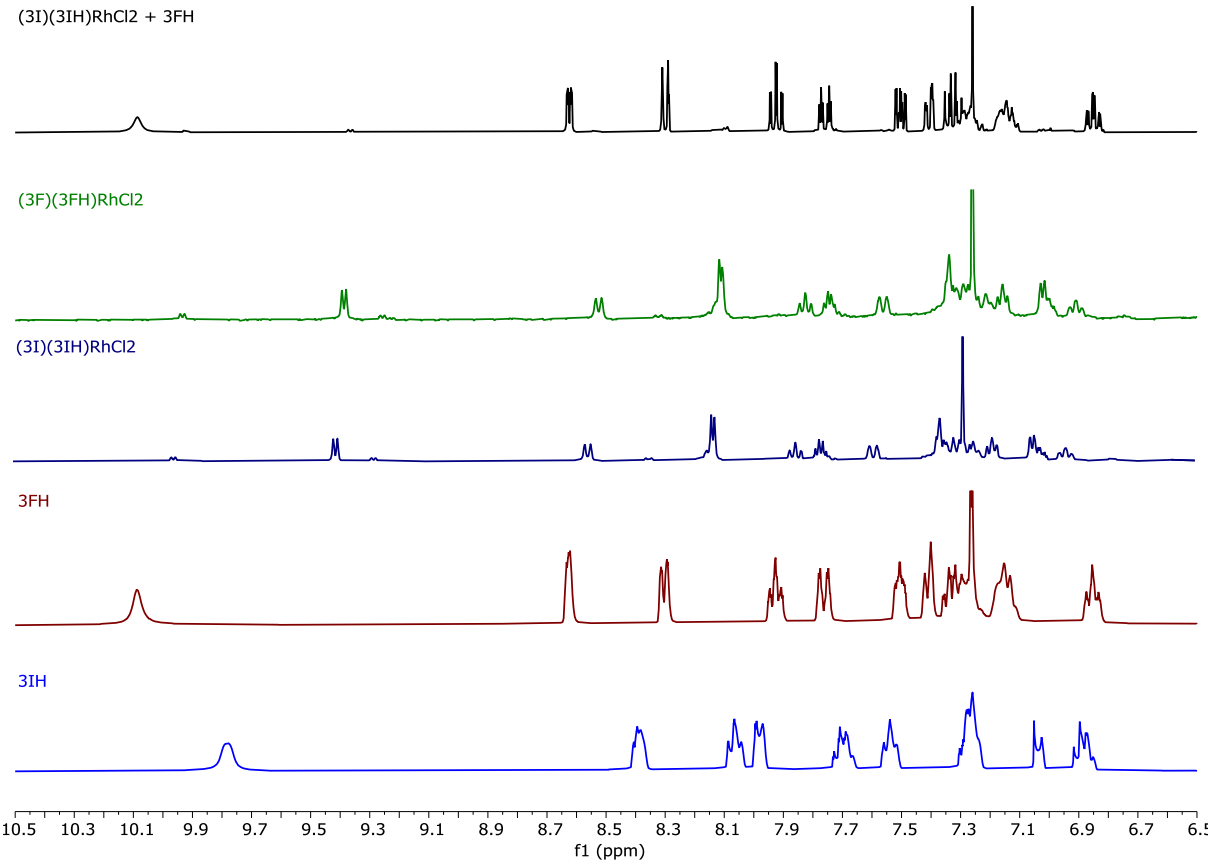

Figure S 10 Overlay of the product (**black**) from the reaction of **[(3'-I)(3'-IH)RhCl$_2$]** (**4**, **dark blue**) + 3'-FH (**dark red**). The spectra for **[(3'-F)(3'-FH)RhCl$_2$]** (**1**, **dark green**) and **3'-IH** (**blue**) are also included for comparison ($CDCl_3$, 300 K, 400 MHz).

The ^{1}H NMR study of an equimolar mixture of **[(3'-I)(3'-IH)RhCl$_2$] (4)** and ***N*-(3-fluorophenyl)picolinamide (3'-IH)** in $CDCl_3$ confirms that the ***N*-(3-fluorophenyl)picolinamide** is the ligand which is most easily substituted, and that the formation of the complex **[(3'-I)(3'-IH)RhCl$_2$] (4)** is energetically favoured. The spectrum of the mixture shows essentially only the resonances of the added ***N*-(3-fluorophenyl)picolinamide** ligand, as the resonances of [(3'-X)(3'-XH)RhCl$_2$] are again "swamped" by the free ligand due to the complex's poor solubility in $CDCl_3$. No resonances of liberated ***N*-(3-fluorophenyl)picolinamide** can be observed.

Complex 5 + N-(3-iodophenyl)picolinamide

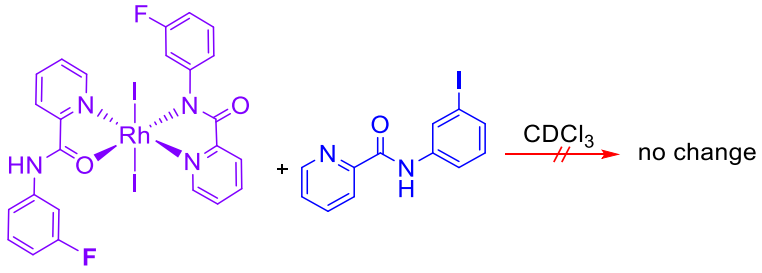

Scheme S3 Test reaction for the ligand exchange between **[(3'-F)(3'-FH)RhI$_2$]** (**5**) with **3'-IH** in $CDCl_3$.

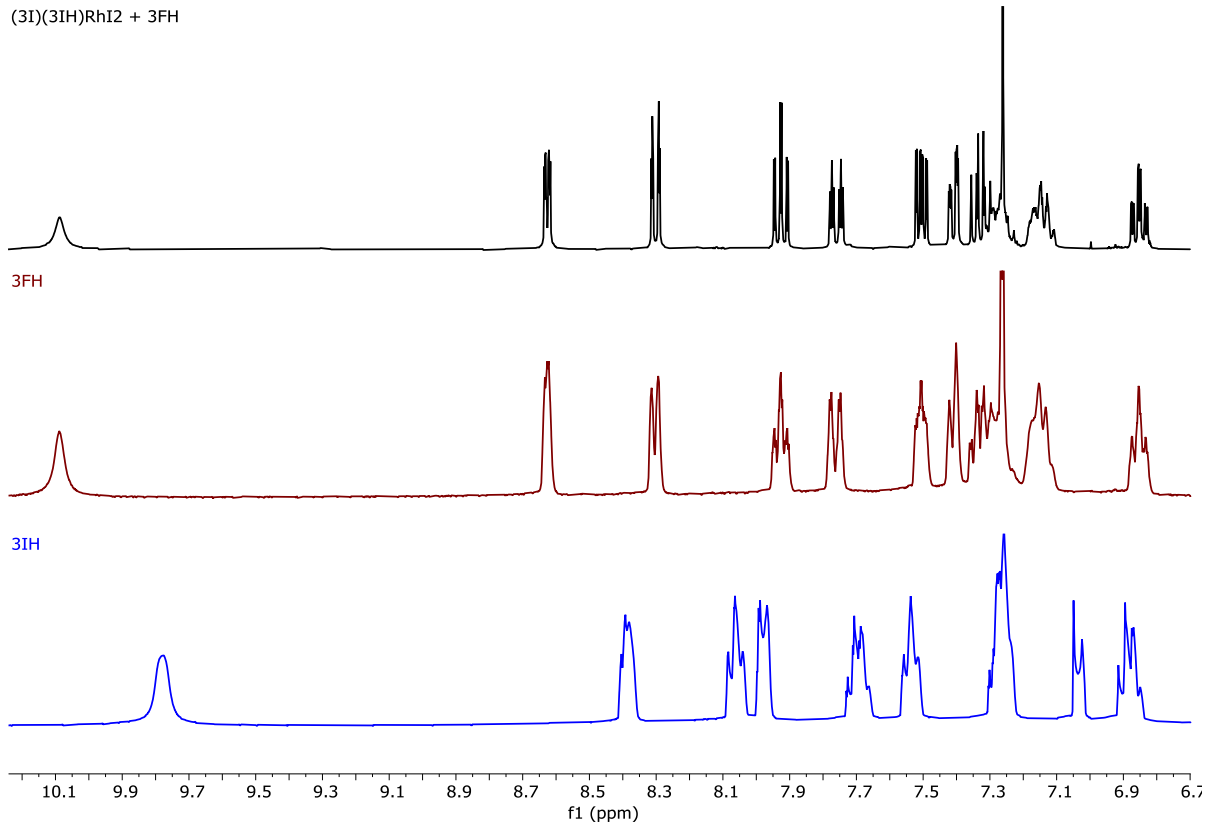

Figure S 11 Overlay of the product (**black**) from the reaction of **[(3'-F)(3'-FH)RhI2]** (**5**) + **3'-IH** (**blue**) The spectra for ligand **3'-FH** (**dark red**) is also included for comparison ($CDCl_3$, 300 K, 400 MHz).

The ^{1}H-NMR study of an equimolar mixture of **[(3'-F)(3'-FH)RhI$_2$]** (**5**) and ***N*-(3-iodophenyl)picolinamide (3'-IH)** in $CDCl_3$ shows free **3'-IH** exclusively. No ligand exchange can be observed as no resonances of liberated ***N*-(3-fluorophenyl)picolinamide (3'-FH)** are present. The extremely poor solubility of **[(3'-F)(3'-FH)RhI$_2$]** in $CDCl_3$ does not allow for a direct comparison of **[(3'-F)(3'-FH)RhI$_2$]** (**5**) and **[(3'-I)(3'-IH)RhI$_2$]** (**8**) and a mixed complex **[(3'-F)(3'-IH)RhI$_2$]** in this solvent. Therefore, the spectra for complex **[(3'-I)(3'-IH)RhI$_2$]** (**8**) + **3'-FH** was not recorded.

NMR's in Dimethyl sulfoxide

Complex 1 + N-(3-iodophenyl)picolinamide

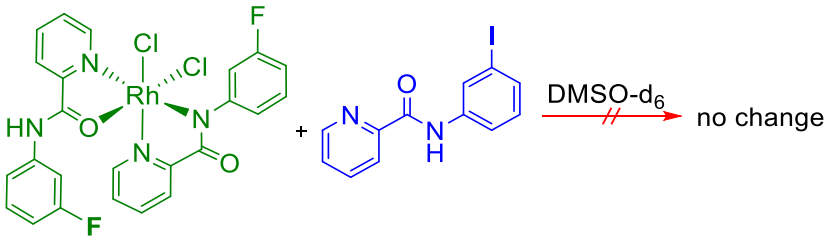

Scheme S4 Test reaction for the ligand exchange between **[(3'-F)(3'-FH)RhCl$_2$]** (**1**) with **3'-IH** in d$_6$-DMSO.

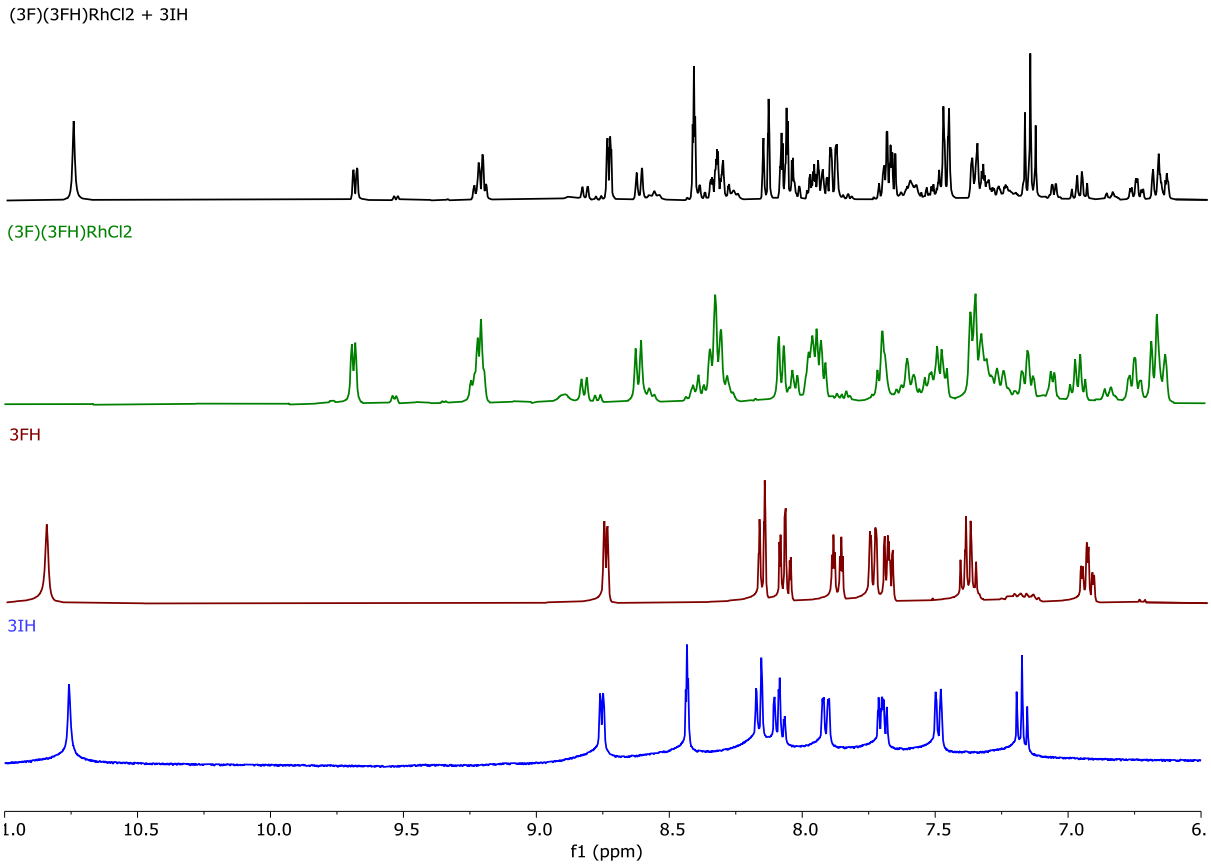

Figure S 12 Overlay of the product (**black**) from the reaction of **[(3'-F)(3'-FH)RhCl$_2$]** (**1**, **dark green**) + **3'-IH** (**blue**). The spectra for ligand **3'-FH** (**dark red**) is also included for comparison (d$_6$-DMSO, 300 K, 400 MHz).

The ^{1}H-NMR study of an equimolar mixture of **[(3'-F)(3'-FH)RhCl$_2$] (1)** and ***N*-(3-iodophenyl)picolinamide (3'-IH)** in d$_6$-DMSO shows no changes in the resonances of the starting material and only an additional set of resonances for the free **3'-IH**. No resonances of free **3'-FH** can be observed, indicating no ligand exchange for **[(3'-L)(3'-LH)RhCl$_2$]** complexes in DMSO.

Complex 5 + N-(3-iodophenyl)picolinamide

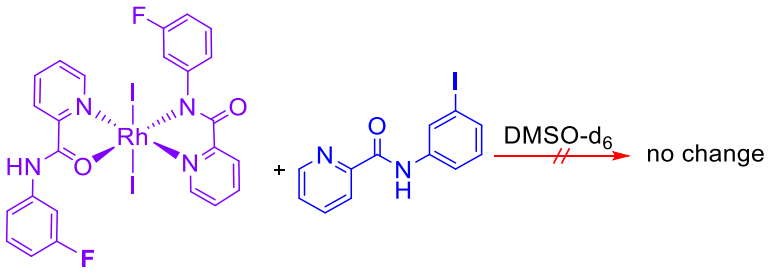

Scheme S5 Test reaction for the ligand exchange between **[(3'-F)(3'-FH)RhI$_2$]** (**5**) with **3'-IH** in d$_6$-DMSO.

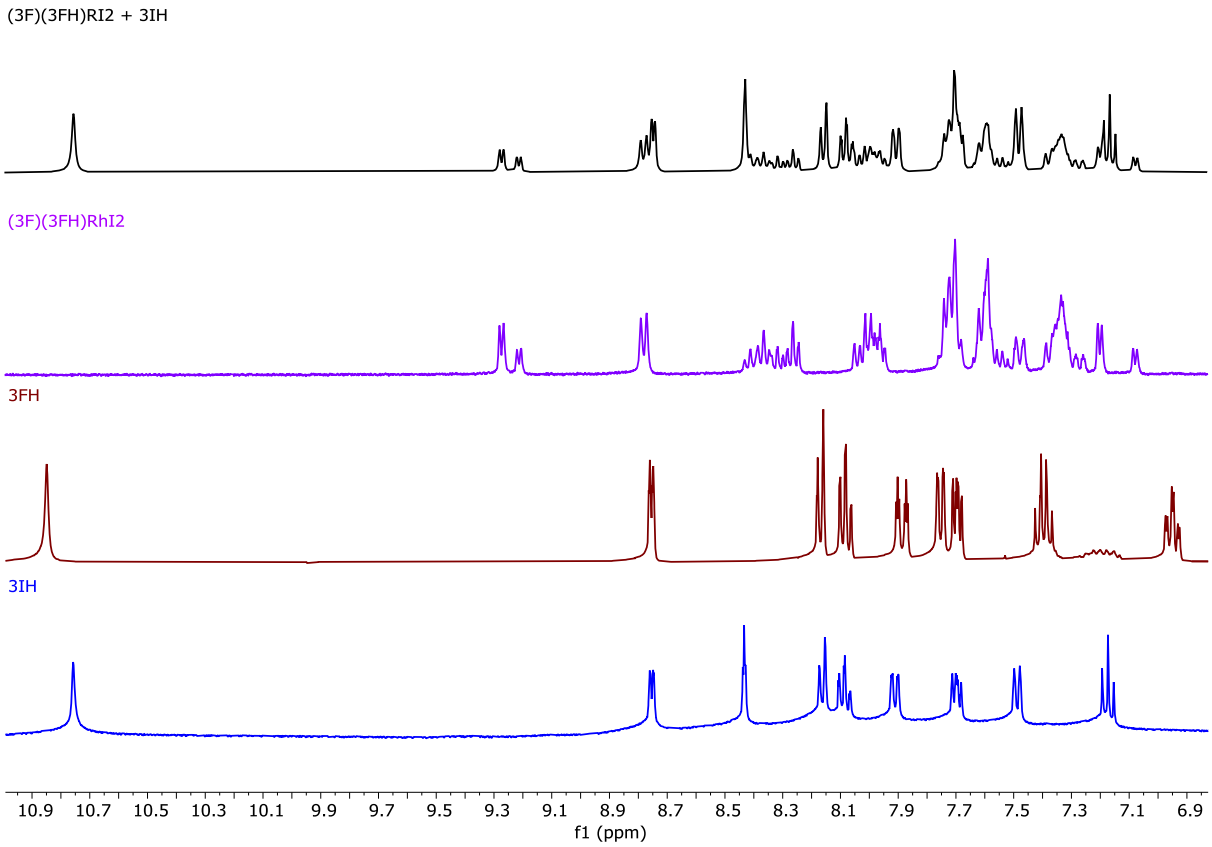

Figure S 13 Overlay of the product (**black**) from the reaction of **[(3'-F)(3'-FH)RhI2]** (**5**) + **3'-IH** (**blue**) The spectra for ligand **3'-FH** (**dark red**) is also included for comparison (d$_6$-DMSO, 300 K, 400 MHz).

The ^{1}H-NMR study of an equimolar mixture of **[(3'-F)(3'-FH)RhI$_2$] (5)** and ***N*-(3-iodophenyl)picolinamide (3'-IH)** in d$_6$-DMSO confirms that complexes of the type **[(3'-L)(3'-LH)RhI$_2$]** do not undergo ligand exchange in DMSO. Along with the resonances of the starting material an additional set of resonances for the free **3'-IH** can be seen, with no resonances of free **3'-FH**, further indicating a lack of ligand exchange in solution.

Stability and Ligand Exchange Studies of Complex 3 and 7 over 96 h

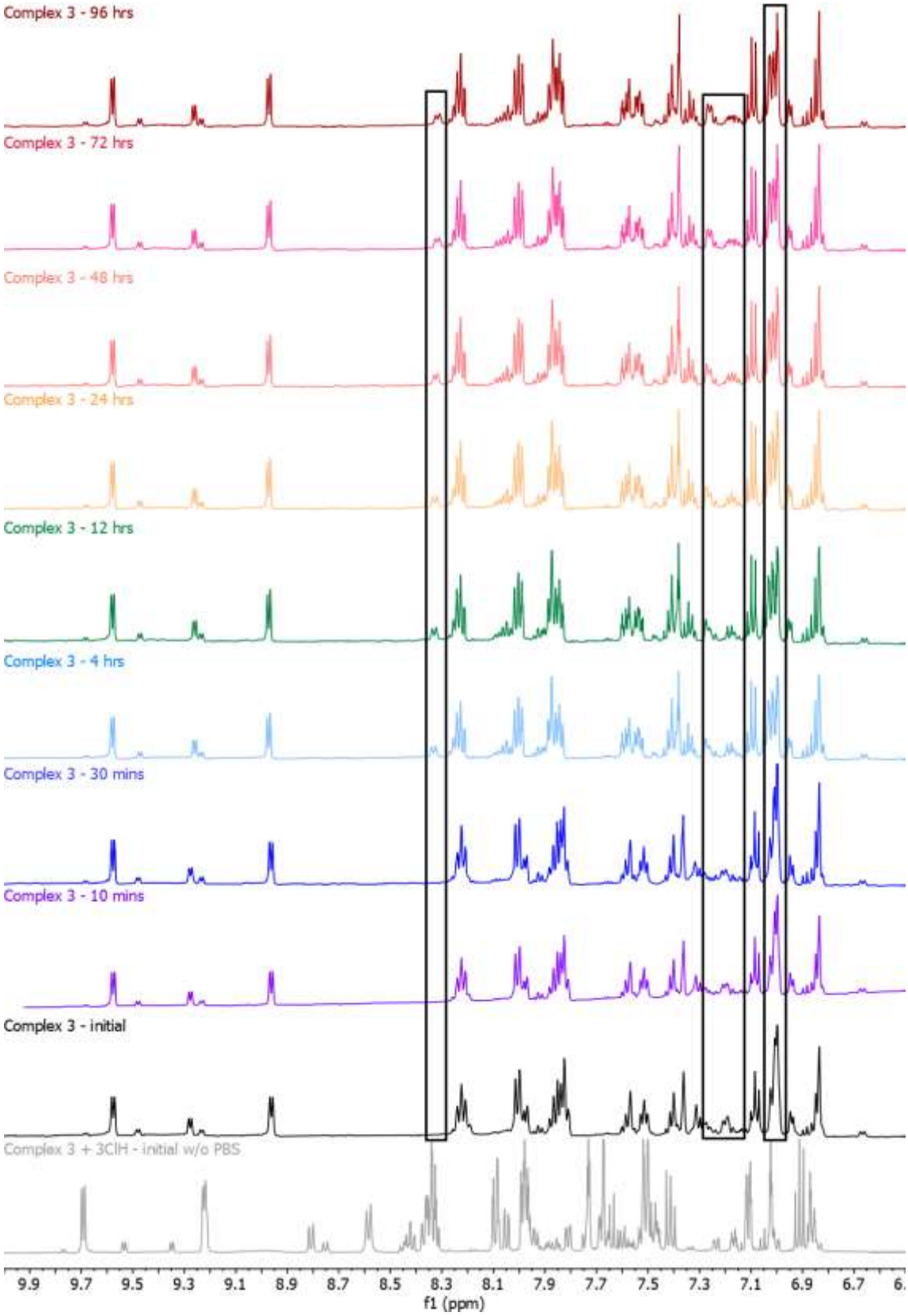

Figure S 14 Stability study of complex **3** in DMSO:PBS (80:20 v/v) over 96 h (d_6-DMSO, 300 K, 400 MHz).

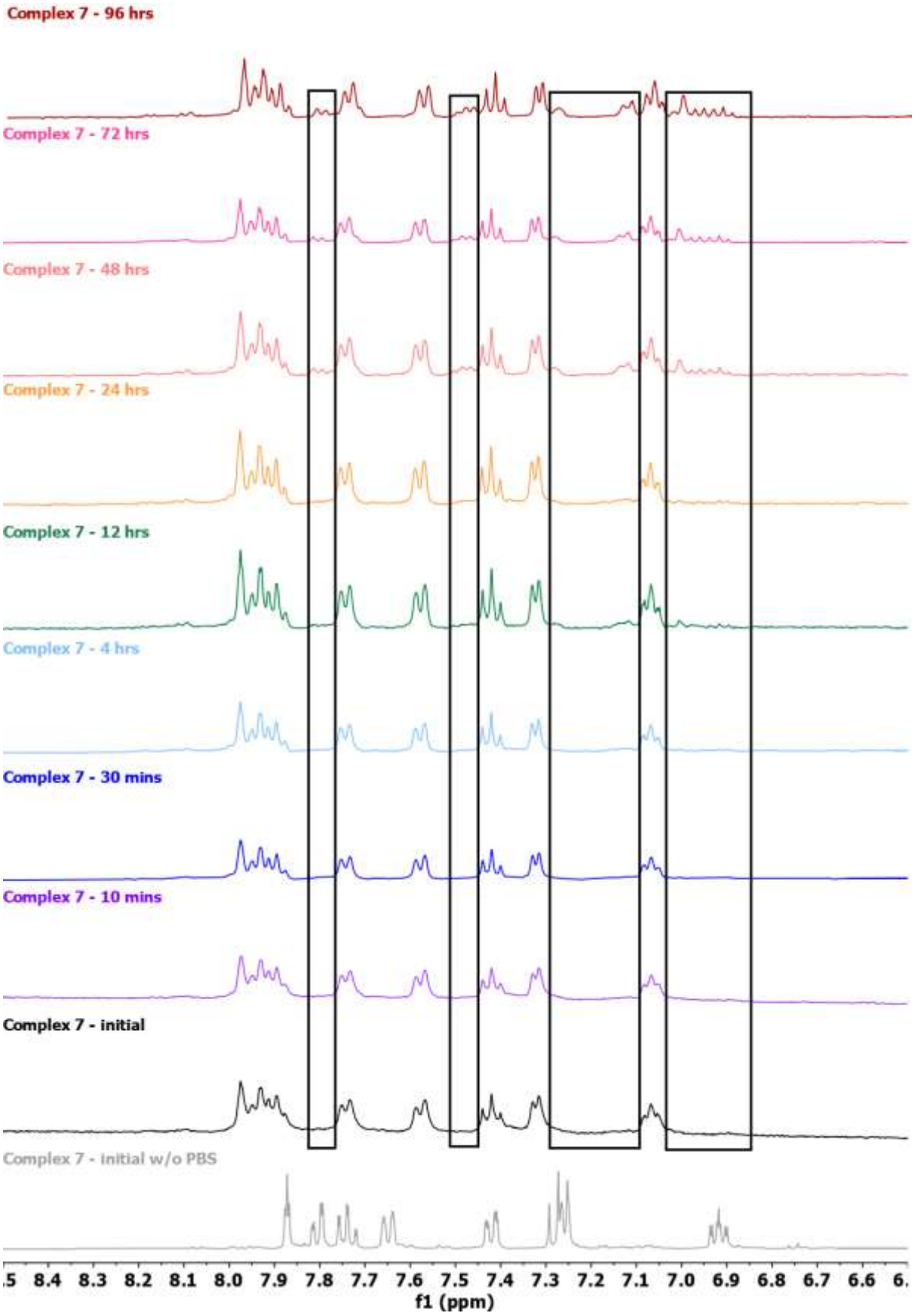

Figure S 15 Stability study of complex **7** in MeCN:PBS (80:20 *v/v*) over 96 h (d_3-MeCN, 300 K, 400 MHz).

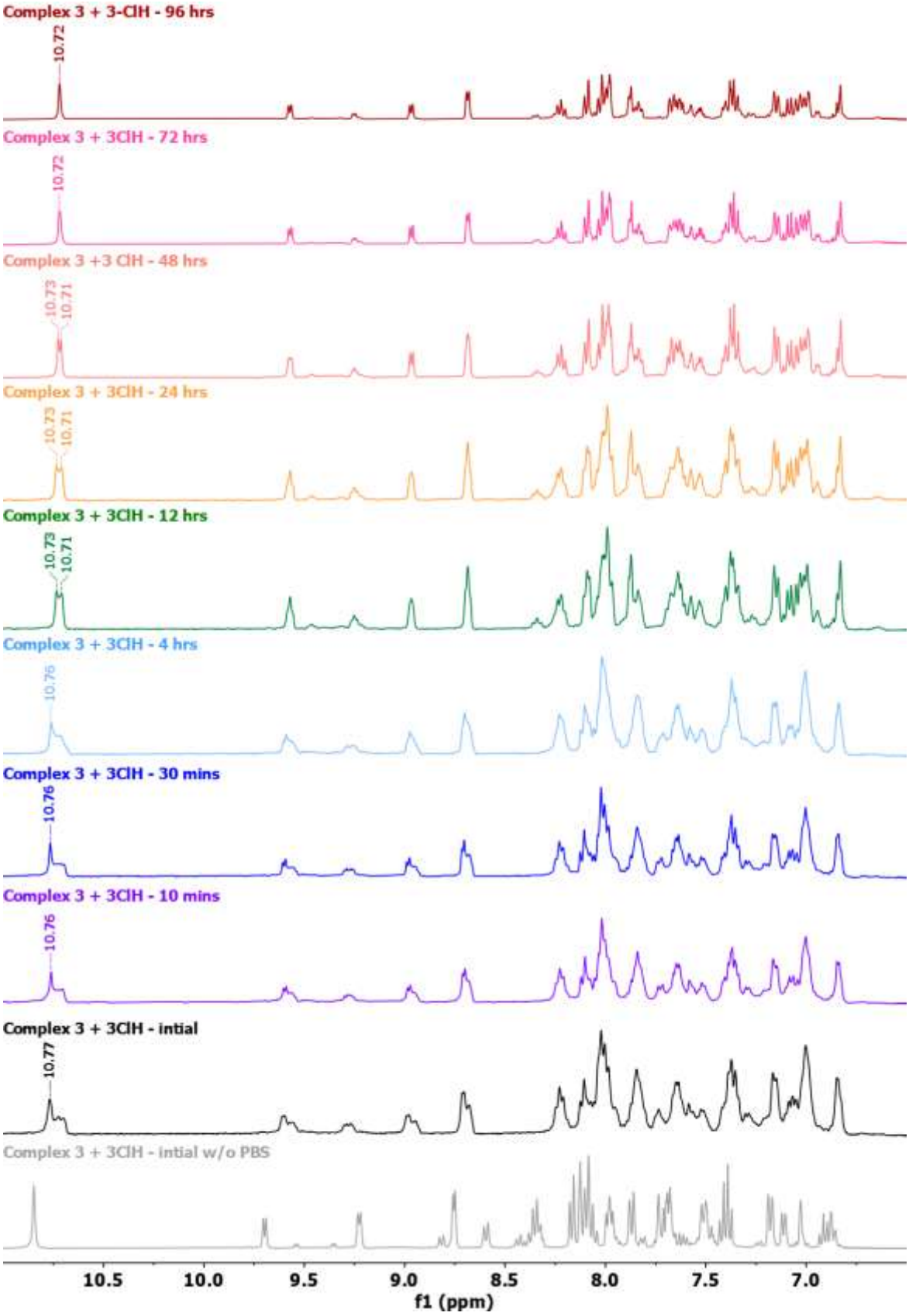

Figure S 16 Exchange studies of complex **3** with *N*-(3-chlorophenyl)picolinamide ligand (**L'**) in DMSO:PBS (80:20 *v/v*) over 96 h (d_6-DMSO, 300 K, 400 MHz).

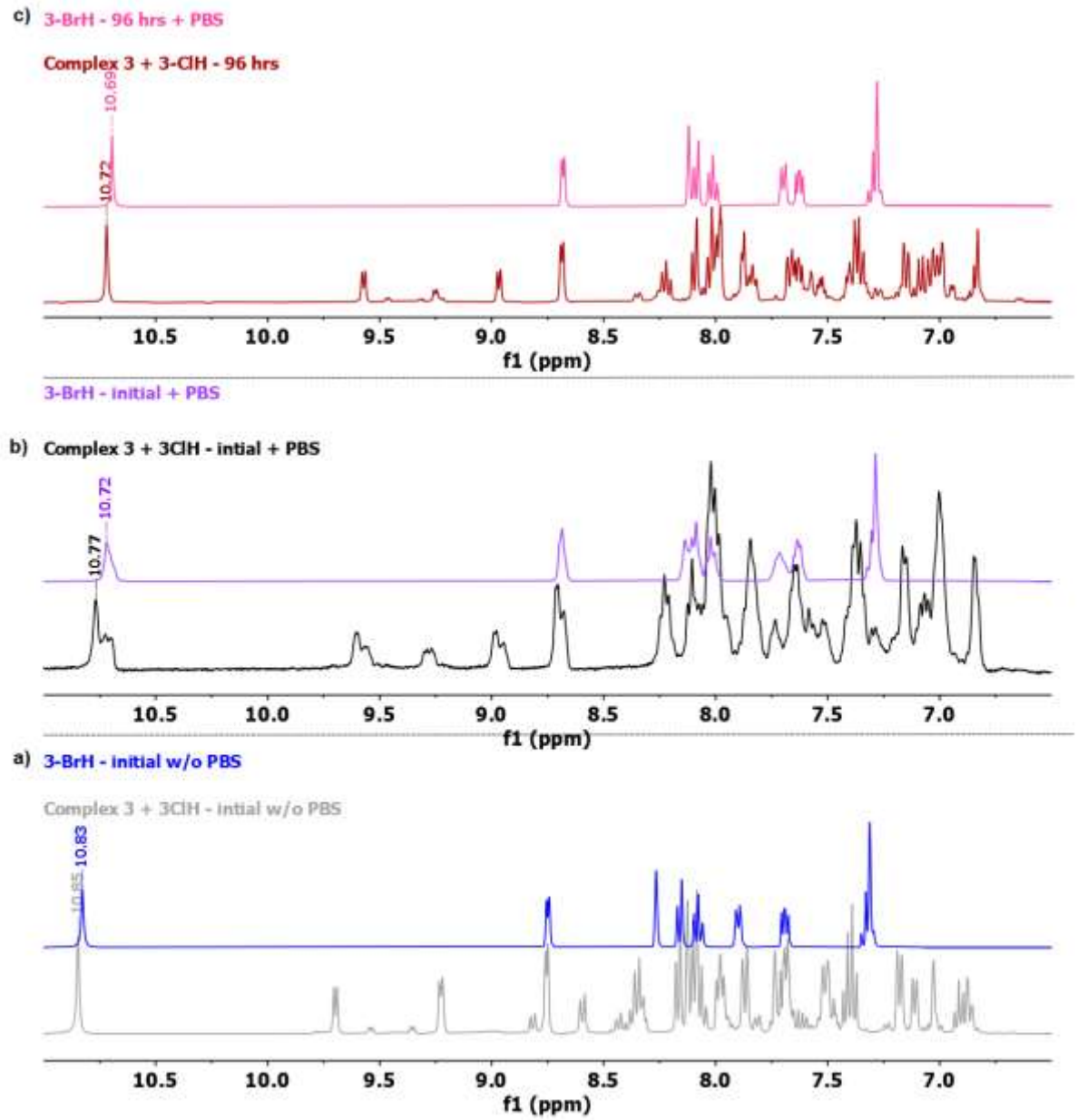

Figure S 17 Overlay of complex **3** and 3'-BrH in MeCN a) without PBS, b) with PBS (80:20 v/v) after initial and c) with PBS (80:20 v/v) after 96 h (d_3-MeCN, 300 K, 400 MHz).

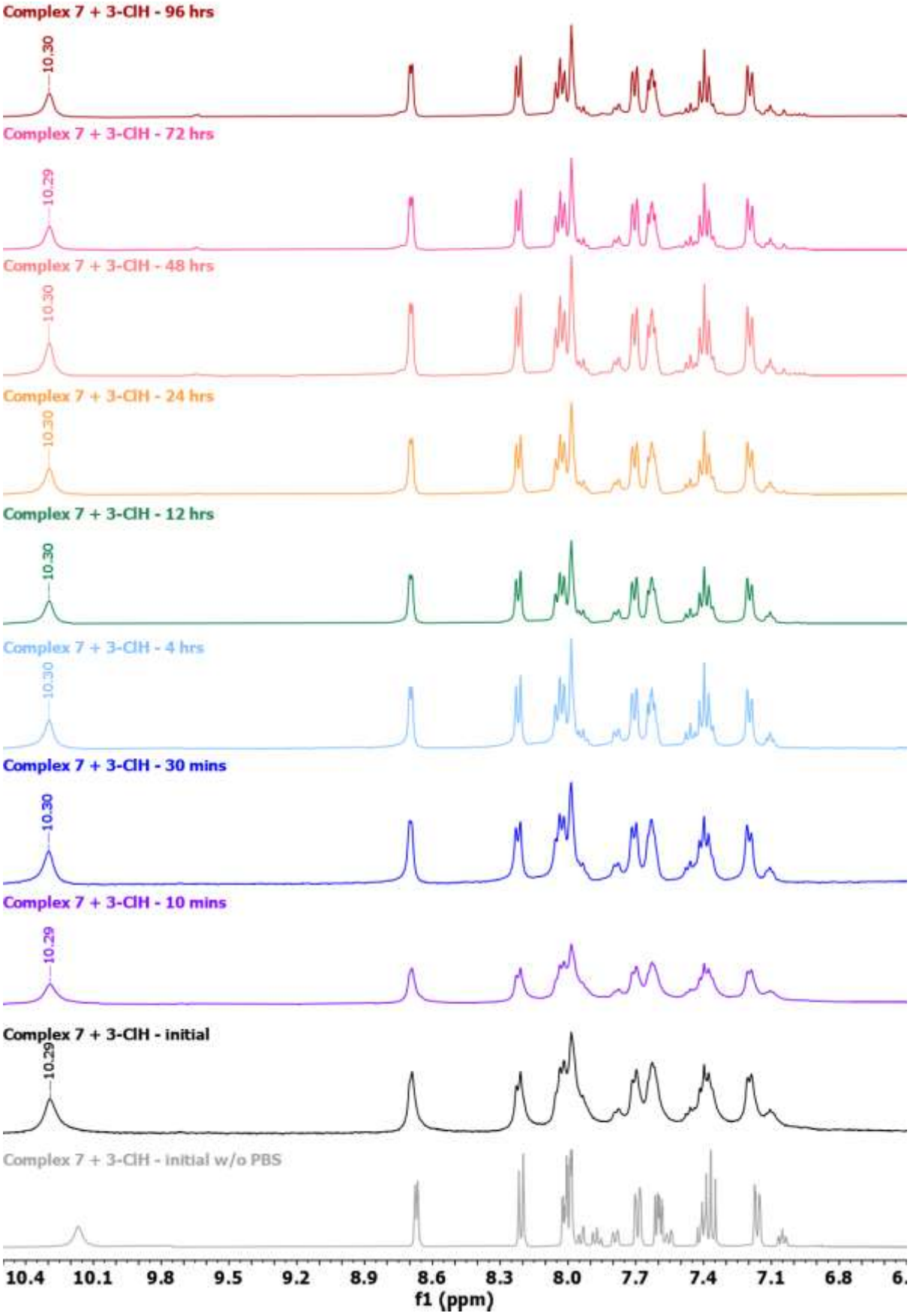

Figure S 18 Exchange studies of complex **7** with *N*-(3-chlorophenyl)picolinamide ligand (**L'**) in MeCN:PBS (80:20 *v/v*) over 96 h (d_3-MeCN, 300 K, 400 MHz).

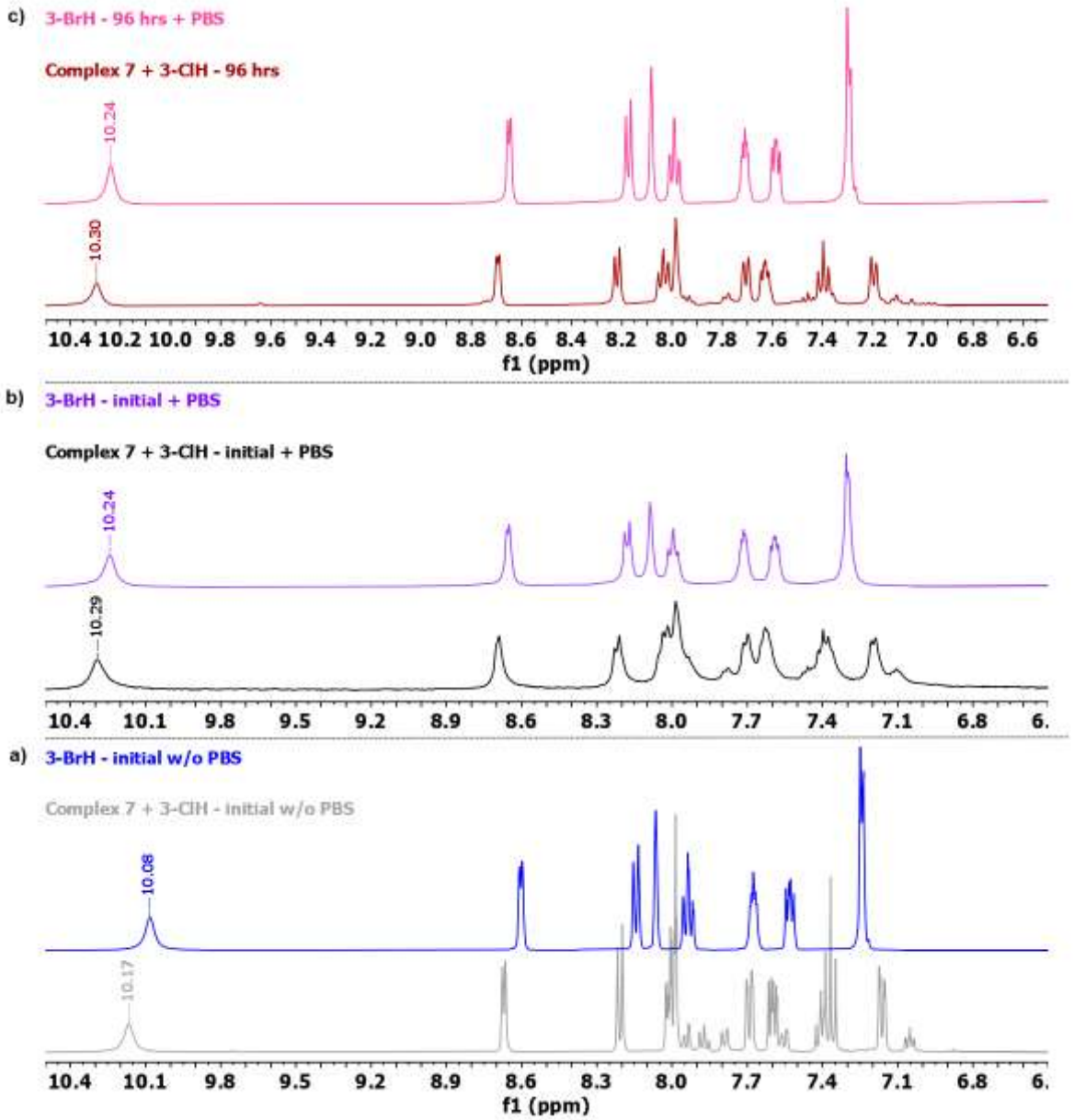

Figure S 19 Overlay of complex **7** and 3'-BrH in MeCN a) without PBS, b) with PBS (80:20 v/v) after initial and c) with PBS (80:20 v/v) after 96 h (d_3-MeCN, 300 K, 400 MHz).

96 h Chemosensitivity Studies

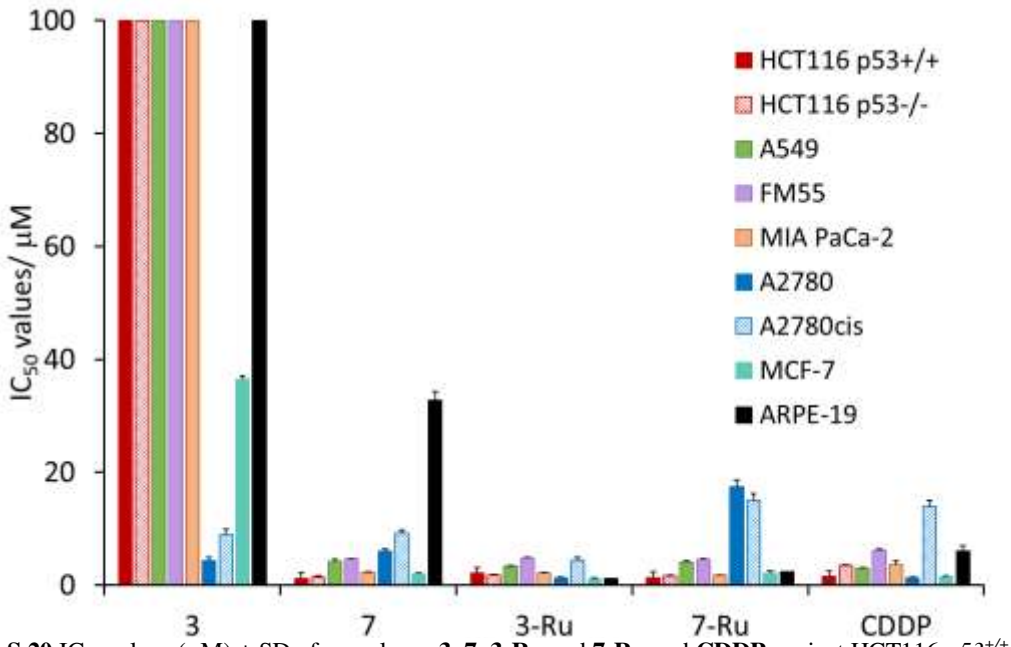

Figure S 20 IC_{50} values (µM) ± SD of complexes **3**, **7**, **3-Ru** and **7-Ru** and **CDDP** against HCT116 *p53*$^{+/+}$, HCT116 *p53*$^{-/-}$, A549, FM55, MIA PaCa-2, A2780, A2780cisR, MCF-7 and ARPE-19.

24 and 72 h Chemosensitivity Studies

Table S 5 IC_{50} values (µM) ± SD for complexes **3**, **7**, **3-Ru**, **7-Ru** and **CDDP** against HCT116 *p53*$^{+/+}$, HCT116 *p53*$^{-/-}$, and ARPE-19, after 24 h and 72 h incubation periods.

Complexes	IC_{50} values (µM) ± SD					
	HCT116 *p53*$^{+/+}$		HCT116 *p53*$^{-/-}$		ARPE-19	
	24 h	72 h	24 h	72 h	24 h	72 h
3	>100	>100	>100	>100	>100	>100
7	1.7 ± 0.1 (21.8)	1.33 ± 0.08 (27.8)	>100 (< 0.4)	>100 (< 0.4)	37 ± 1	33 ± 1
3-Ru	2.1 ± 0.2 (1.1)	2.02 ± 0.08 (1.2)	2.3 ± 0.2 (1.0)	2.10 ± 0.09 (1.1)	2.41 ± 0.07	2.2 ± 0.3
7-Ru	1.7 ± 0.1 (1.6)	1.29 ± 0.05 (2.1)	4.3 ± 0.1 (0.6)	4.07 ± 0.07 (0.7)	2.7 ± 0.2	2.5 ± 0.3
CDDP	77 ± 2 (0.5)	71.6 ± 0.4 (0.6)	>100 (< 0.4)	>100 (< 0.4)	41 ± 1	37 ± 1

Selectivity Factors (SF)

Table S 6 Selectivity Factors (SF) for complexes **7**, **3-Ru**, **7-Ru** and **CDDP** when comparing the IC_{50} values of the isogenic colorectal cancer cell lines (HCT116 $p53^{+/+}$ and HCT116 $p53^{-/-}$) after 24, 72 and 96 h incubation periods.

Complexes	SF towards HCT116 $p53^{-/-}$			SF towards HCT116 p53+/+		
	24 h	72 h	96 h	24 h	72 h	96 h
7	0.02	0.01	0.90	57.47	75.16	1.11
3-Ru	0.92	0.96	1.20	1.09	1.04	0.83
7-Ru	0.38	0.32	0.80	2.61	3.16	1.26
CDDP	0.77	0.72	0.42	1.30	1.40	2.36

LogP, Solubility and Pharmacokinetics

Table S 7 Predictions of logP, solubility and pharmacokinetics for complexes 1-8, 3-Ru and 7-Ru, using Swiss ADME.[1]

Complex	Log P (MLOG)	LogS (ESOL)	Solubility mg/ mL	Class	GI absorption	Pharmacokinetics
1	3.54	-8.33	$2.83x10^{6}$	Poorly soluble	High	P-gp substrate, CYP1A2 inhibitor, CYP2C19 inhibitor
2	3.91	-8.75	$1.16x10^{6}$	Poorly soluble	High	BBB permeant, P-gp substrate, CYP3A4 inhibitor
3	4.10	-9.38	$3.07x10^{7}$	Poorly soluble	High	BBB permeant, P-gp substrate
4	4.29	-9.91	$1.02x10^{7}$	Poorly soluble	High	BBB permeant, P-gp substrate
5	4.10	-9.09	$6.48x10^{7}$	Poorly soluble	High	BBB permeant, P-gp substrate
6	4.29	-9.96	$9.19x10^{8}$	Poorly soluble	High	BBB permeant, P-gp substrate
7	4.48	-10.59	$2.38x10^{8}$	Insoluble	High	P-gp substrate
8	4.67	-11.12	$7.66x10^{9}$	Insoluble	High	BBB permeant, P-gp substrate
3-Ru	4.10	-9.37	$3.15x10^{7}$	Poorly soluble	High	BBB permeant, P-gp substrate
7-Ru	4.48	-10.58	$2.43x10^{8}$	Insoluble	Hugh	P-gp substrate

References

(1) Daina, A.; Michielin, O.; Zoete, V. SwissADME: A Free Web Tool to Evaluate Pharmacokinetics, Drug-Likeness and Medicinal Chemistry Friendliness of Small Molecules. *Sci Rep* **2017**, *7* (Article number: 42717). https://doi.org/10.1038/srep42717.